phys. stat. sol. (c), 1–5 (2005) / **DOI** 10.1002/pssc.200461480

Heterojunctions between group-III nitride short-period superlattices

K. A. Bulashevich[*1,2] and **S. Yu. Karpov**[1]

[1] Soft-Impact, Ltd., P.O. Box 83, 27 Engels av., St. Petersburg 194156, Russia
[2] Ioffe Physico-Technical Institute, RAS, 26 Polytekhnicheskaya, St. Petersburg 194021, Russia

Received 12 July 2004, revised 8 February 2005, accepted 21 February 2005
Published online 1 April 2005

PACS 73.21.Cd, 73.40.Kp, 78.67.Pt, 85.60.Jb

Group-III nitride short-period superlattices (SPSLs) and heterojunctions between them are studied theoretically in terms of the parameters, normally invoked for bulk materials. Relationships between the SPSL structure and their macroscopic characteristics, bandgap, band offsets, and polarization, are considered. The SPSL bandgap is found to depend directly on the quantum-well width/composition and on the barrier width/composition via competition between the quantum-confinement Stark effect (QCSE) and miniband broadening. The mean (period-averaged) electric field is shown to break at the SPSL heterojunction. The break depends on the difference in the SPSL macroscopic polarization which is similar to the spontaneous polarization of bulk nitride materials. In contrast to bulk semiconductors, the bandgap and macroscopic polarization of a SPSL can be controlled independently by adjusting the well/barrier width and composition. A light emitting diode (LED) heterostructure containing SPSL regions is discussed to illustrate the contact phenomena occurring at the SPSL junctions.

1 Introduction For a long time, short-period superlattices serve as important elements of a heterostructure design, aimed at solving either technological or design problems. In the case of group-III nitrides, SPSLs have been used for reduction of dislocation density in epitaxial materials (see, e.g. [1,2]), enhancement of Mg acceptor activation [3,4], increase of hole injection efficiency [5], and even as n- and p-emitters and active regions in light emitting diodes and laser diodes [6–8]. In all the above cases, specific electronic properties of SPSLs like existence of mini-gaps in the conduction and valence bands or negative differential resistance are not exploited. Instead, a SPSL is considered as a bulk material with anisotropic properties which can be controlled by its internal microscopic parameters – thicknesses and compositions of constituent layers and their doping. Though properties of individual nitride superlattices have been already started to study [3,4,8–10], the contact phenomena at the interfaces between either different SPSLs or a bulk material and a SPSL are not yet examined at all.

In this study, an attempt is made to describe, at least qualitatively, a junction between two nitride SPSLs in terms of parameters normally invoked for bulk heterojunctions – bandgaps and interface polarization charges. We will examine these parameters as a function of SPSL microscopic structure, i.e. widths and compositions of the quantum well (QW) and barrier layers. An SPSL LED heterostructure is considered to illustrate contact phenomena occurring at the SPSL junctions.

2 Electric field and macroscopic polarization The electric potential distribution in a nitride SPSL is controlled by a polarization charge alternating on the superlattice interfaces rather than by a spatial

* Corresponding author: e-mail: kirill@softimpact.ru, Phone: +7 (812) 554 4570, Fax: +7 (812) 326 6194

charge of free carriers and ionized impurities. Without external field applied, the potential drop across the SPSL period equals zero, and the electric fields in the QW, F_{W}, and barrier, F_{B}, are

$$F_{\mathrm{W}} = \frac{\sigma}{\varepsilon\varepsilon_0}\frac{d_{\mathrm{B}}}{d_{\mathrm{W}}+d_{\mathrm{B}}} \quad \text{and} \quad F_{\mathrm{B}} = -\frac{\sigma}{\varepsilon\varepsilon_0}\frac{d_{\mathrm{W}}}{d_{\mathrm{W}}+d_{\mathrm{B}}} \ . \tag{1}$$

Here, d_{W} and d_{B} are the widths of the QW and barrier, respectively, ε_0 is the dielectric permittivity of vacuum, ε is the dielectric constant assumed to be the same for QWs and barriers, $\sigma = P_{\mathrm{B}} - P_{\mathrm{W}}$ is the polarization charge at the QW interface, P_{W} and P_{B} are the total electric polarizations in the QW and barrier, respectively, accounting for both the spontaneous polarization and piezoeffect.

Consider the band diagram and the electric field distribution near an SPSL junction shown in Fig. 1 for the superlattices differing by the QW widths only. No external field is assumed to exist in the left SPSL, so that the electric fields in the QW and barrier obey Eq. (1). Both SPSLs have the same surface charges at the well/barrier interfaces, providing the same electric fields in the barriers and wells in the left and right SPSLs. However, a wider QW in the right SPSL produces an additional potential drop across its period, resulting in noticeable mean (averaged over the SPSL period) electric field. Extending this consideration to the case of two SPSLs of arbitrary parameters, we can derive the general relationship between the mean electric fields $\widetilde{F}$ on both sides of the SPSL junction

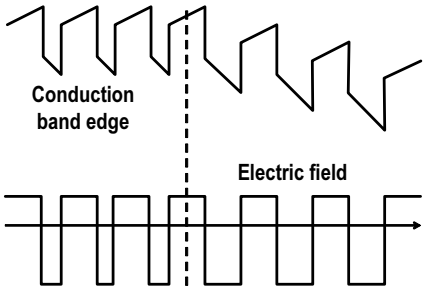

Fig. 1 Schematic view of the SPSL heterojunction.

$$\widetilde{F}_l - \widetilde{F}_r = -\frac{\widetilde{P}_l - \widetilde{P}_r}{\varepsilon\varepsilon_0} \ , \quad \text{where} \quad \widetilde{P} = \frac{P_{\mathrm{W}}d_{\mathrm{W}} + P_{\mathrm{B}}d_{\mathrm{B}}}{d_{\mathrm{W}}+d_{\mathrm{B}}} \tag{2}.$$

Equation (2) can be interpreted in terms of a polarization charge located on the interface between two connected SPSLs and equal to the difference of the macroscopic polarizations $\widetilde{P}$ attributed to these SPSLs. It is important that Eq. (2) is independent of the way of SPSL conjunction (barrier-to-barrier or barrier-to-well) and remains valid even if a transition layer is inserted between the SPSLs.

3 Carrier density calculation To compute the equilibrium distribution of the electric potential and carrier concentration in the SPSL, we solve the Poisson equation for the SL period with periodic boundary conditions for potential and electric field, coupled with the following calculation of the majority carrier density. Below we will describe the calculations for electrons, and the same approach is used for each type of holes. First, we compute the ground energy level E_0 for the individual QW by numerical solution of the Schrödinger equation with an effective potential presented in Fig. 2, which coincides the conduction band in one SL period and equals the barrier maximum outside. Then we calculate the resonance integral J and overlap integral S and obtain the electron dispersion relation within the tight-binding approximation

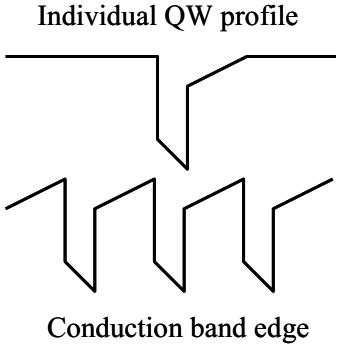

Fig. 2 Individual QW profile.

$$E(k_\perp, k_\parallel) = E_0 + \frac{\hbar^2 k_\parallel^2}{2m_\parallel^{QW}} - \frac{2J\cos(k_\perp d)}{1+2S\cos(k_\perp d)} \ , \tag{3}$$

where $m_\parallel^{QW}$ is the electron in-plane effective mass in the QW layer. The electron concentration is calculated by integrating the product of the density of states found from Eq. (3) and Fermi distribution func-

tion. The higher miniband contribution to the carrier density was evaluated in the same way.

4 Bandgap It is natural to define the SPSL bandgap as the separation between the electron ground miniband bottom and the higher hole miniband top. The bandgap depends both on the energy levels in individual QWs and coupling of the adjacent QWs resulting in miniband formation

$$E_{\mathrm{g}}^{\mathrm{SL}} = E_0^e - E_0^h - \frac{2J^e}{1+2S^e} - \frac{2J^h}{1+2S^h} \quad , \qquad (4)$$

where superscripts e and h correspond to electrons and holes of the top miniband, respectively.

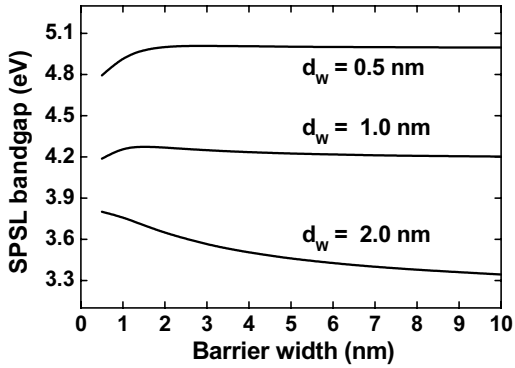

Fig. 3 Effective $Al_{0.1}Ga_{0.9}N$/AlN SPSL bandgap as a function of the barrier width.

Figure 3 shows the bandgap of unintentionally doped $Al_{0.1}Ga_{0.9}N$/AlN SPSL as a function of barrier width computed for different thicknesses of the QW layer. The SPSL bandgap depends primarily on the QW width which significantly changes the energy levels. However, the bandgap variation with the barrier width can be non-monotonic because of the competition between the quantum-confined Stark effect (QCSE) and miniband broadening. Indeed, the electric field in QW rises with the barrier width according to Eq. (1), which results in a decrease of the SPSL bandgap due to the QCSE. On the other hand, the wider the barrier, the less pronounced is the effect of the bandgap narrowing due to miniband formation. The barrier composition variation also affects contrariwise the miniband formation and QCSE. The minibands become narrower at a higher AlN content in the barrier, while the electric field in the QW rises due to a greater surface charge σ. Since the red shift due to the QCSE increases rapidly with the QW width, we can conclude that the bandgap increases with the barrier width in the SPSLs with narrow QWs and decreases in the case of wide QWs (see Fig. 3).

5 SPSL LED double heterostructure Recently, UV LEDs of various designs employing p-n junctions between different SPSLs have been demonstrated [7,8]. In particular, it has been shown that the use of an i-SPSL active region with a wider quantum wells between the n- and p-doped SPSL claddings increases the emission intensity compared to an LED consisting of the n- and p-SPSLs only. Actually, such a p-i-n LED operates like a conventional double heterostructure (DHS) device [8]. Indeed, the bandgap of the SPSL with wider quantum wells is lower than those of the claddings, producing better carrier localization inside the active region and, hence, a higher internal emission efficiency.

To obtain the band diagrams, we solve the Poisson equation coupled with the calculation of the carrier density described in Sec. 3. The electron and hole Fermi levels are assumed to be constant and their separation is suggested to be equal to the bias applied. The boundary conditions are electroneutrality of the first and last SL periods. The results for the p-n and p-i-n $Al_{0.1}Ga_{0.9}N$/AlN SPSL LEDs are shown in Fig. 4. The barrier widths in the all the SPSLs are 1 nm, while the QW width is 1 nm in the DHS active region and 0.5 nm in the n- and p-claddings. The impurity concentration of 1×10^{19} cm^{-3} is taken in both n- and p-regions.

Figure 4 illustrates a close similarity between the SPSL based devices and their bulk prototypes. The effective surface charges are formed at the interfaces of the DHS active region where the mean electric field is directed opposite to the built-in field of the p-n junction. Such a behavior is typical to conventional single-quantum well (SQW) InGaN LED heterostructures with polarization charges on the SQW interfaces. In the case of p-n SPSL junction, no effective surface charges are observed due to the equal macroscopic polarizations in both n- and p-SPSLs. Thus, the p-n SPSL LED is quite similar to ordinary p-n junction diode.

6 Conclusion In this paper, we have considered the contact phenomena occurring at SPSL junctions in terms of the parameters normally invoked for bulk heterostructures. Close similarity in the behaviour of the bulk and SPSL LED structures is demonstrated. It is important that the key SPSL parameters, macroscopic polarization and bandgap, can be controlled independently by adjusting the thicknesses and compositions of SPSL constituent layers. This opens new opportunities for optimization of the device heterostructures. The analogy between the SPSL and bulk heterojunctions may serve as a guideline for the bandgap engineering of the SPSL-based devices.

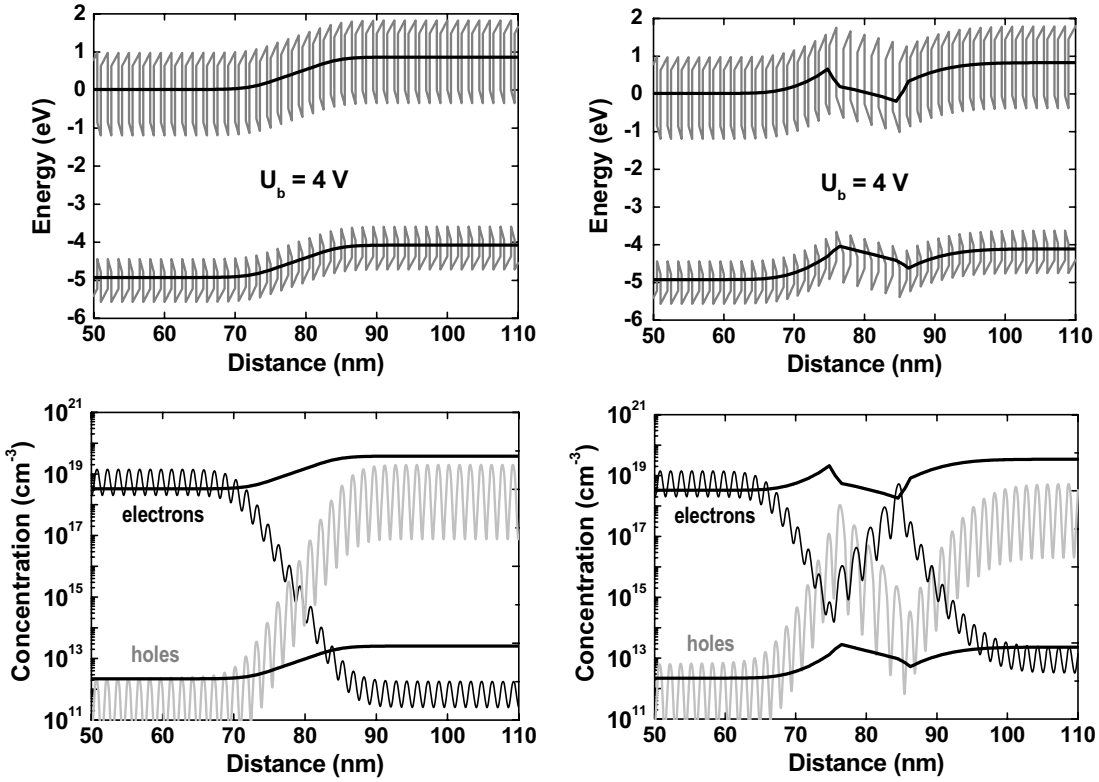

Fig. 4 Band diagrams and concentrations of electrons and heavy holes in p-n SPSL LED (left) and p-i-n DHS SPSL LED (right) at the bias of 4 V. Effective bandgaps are marked by thick black lines.

Acknowledgements The work of K. A. Bulashevich is supported in part by the Russian Federal Program on Support of Leading Scientific Schools, grant 2160.2003.2.

References

[1] H. Hirayama, M. Ainoya, A. Kinoshita, A. Hirata, and Y. Aoyagi, App. Phys. Lett. **80**, 2057 (2002).
[2] H.-M. Wang, J.-P. Zhang, C.-Q. Chen, Q. Fareed, J.-W. Yang, and M. Asif Khan, Appl. Phys. Lett. **81**, 604 (2002).
[3] E. F. Schubert, W. Grieshaber, and I. D. Goepfert, Appl. Phys. Lett. **69**, 3737 (1996); I. D. Goepfert, E. F. Schubert, A. Osinsky, and P. E. Norris, Electron. Lett. **35**, 1109 (1999).
[4] P. Kozodoy, Y. P. Smorchkova, M. Hansen, H. Xing, S. P. DenBaars, U. K. Mishra, A. W. Saxler, R. Perrin, and W. C. Mitchel, Appl. Phys. Lett. **75**, 2444 (1999).
[5] S. M. Komirenko, K. W. Kim, V. A. Kochelap, and J. M. Zavada, Solid State Electron. **47**, 169 (2003).

[6] S. Nakamura, M. Senoh, S.-i. Nagahama, N. Iwasa, T. Yamada, T. Matsushita, H. Kiyoku, Y. Sugimoto, T. Kozaki, H. Umemoto, M. Sano, and K. Chocho, J. Cryst. Growth **189/190**, 820 (1998).
[7] G. Kipshidze, V. Kuryatkov, K. Zhu, B. Borisov, M. Holtz, S. Nikishin, and H. Temkin, J. Appl. Phys. **93**, 1363 (2003).
[8] G. Kipshidze, V. Kuryatkov, B. Borisov, M. Holtz, S. Nikishin, H. Temkin, Appl. Phys. Lett. **80**, 3682 (2002).
[9] B. K. Ridley, W. J. Schaff, and L. F. Eastman, J. Appl. Phys. **94**, 3972 (2003).
[10] E. L. Waldron, Y.-L. Li, E. F. Schubert, J. W. Graff, and J. K. Sheu, Appl. Phys. Lett. **83**, 4975 (2003).